

THE PHYSICAL REVIEW

A journal of experimental and theoretical physics established by E. L. Nichols in 1893

SECOND SERIES, VOL. 184, No. 3

15 AUGUST 1969

Absolute Experimental X-Ray Form Factor of Aluminum*

P. M. RACCAH AND V. E. HENRICH

Lincoln Laboratory, Massachusetts Institute of Technology, Lexington, Massachusetts 02173

(Received 3 January 1969)

The first nine structure factors of aluminum have been measured on an absolute scale by symmetric x-ray reflection from cold-worked powder pellets. The polarization ratio of the monochromator was measured using the scattering at 90° in 2θ from a perfect Ge crystal. The sample absorption was also measured directly on pressed pellets. The final results confirm the existence of a solid-state effect for the low-order reflections, and show excellent agreement with the free-atom relativistic Hartree-Fock calculation for high-order reflections.

INTRODUCTION

OVER the past thirty years there have been many x-ray diffraction measurements of the charge density in aluminum. Only recently, however, has the accuracy become sufficient to observe the effects of the crystalline potential on the free-atom charge distribution. These effects are expected to represent a perturbation of a few percent; thus an accuracy of $\pm 1\%$ is necessary. At least four measurements fall into that category; those of Bensch, Witte, and Wolfel¹ (BWW), Batterman, Chipman, and DeMarco² (BCD), DeMarco³ (DM), and Järvinen, Merisalo, and Inkinen⁴ (JMI). These were performed on single crystals by transmission, on cold-worked powders by reflection, on single crystals by transmission (using a sophisticated method of correction for secondary extinction), and on cold-worked powders by transmission, respectively. All four are absolute measurements.

The measured form factors are listed in Table I along with the atomic relativistic Hartree-Fock (RHF) values calculated by Doyle and Turner.⁵ In order to make meaningful comparison possible, both BWW and BCD were corrected using the best current values of the Debye temperature (387°K) and the anomalous dispersion (0.04). The JMI results, which are limited

to the first three reflections, are not listed, since their values are not yet published. In their abstract,⁴ agreement with the DM results is claimed.

For the first two reflections [(111) and (200)], it can be seen that all results are lower than the RHF values, and that they are lower than the neon core values, which are obtained by subtracting the contribution of the $3s^23p^1$ electrons from the free-atom scattering factor (column 5). The usual interpretation^{3,5} has been that the $2p^6$ closed shell was expanded in the solid. Weiss⁶ went on to calculate the energy necessary for such a change and found it to be ten times larger (26 eV) than the lattice binding energy (3 eV). This unlikely situation was called the "aluminum dilemma."

The other striking discrepancy in Table I is the disagreement of all experimental results, both with one

TABLE I. Comparison of previous experimental form factors for aluminum.

hkl	k /4π (Å ⁻¹)	Experimental form factor			Relativistic Hartree-Fock theory	
		Bensch, Witte, and Wolfel	Batterman, Chipman, and DeMarco	DeMarco	Alumi- num	Neon core
111	0.2138	8.63±0.13	8.70±0.14	8.69±0.04	8.97	8.87
200	0.2470	8.32±0.08	8.32±0.14	8.21±0.07	8.51	8.54
220	0.3493	7.25±0.07	7.16±0.13	7.25±0.06	7.32	7.39
311	0.4094	6.57±0.07	6.50±0.12		6.66	6.68
222	0.4276	6.49±0.06	6.27±0.13		6.47	6.45
400	0.4937	5.90±0.06	5.56±0.15		5.76	5.74
331	0.5381	5.41±0.08	5.04±0.14		5.32	5.28
420	0.5520	5.46±0.08	4.75±0.13		5.18	5.14
422	0.6047	4.81±0.20	4.46±0.15		4.67	4.62
511	0.6414	4.48±0.18	4.08±0.16	4.28±0.04	4.37	4.32
333	0.6414	4.44±0.18	4.08±0.16	4.26±0.04	4.37	4.32

* Work sponsored by the U. S. Air Force.

¹ H. Bensch, H. Witte, and E. Wolfel, *Z. Physik. Chem. (Leipzig)* **4**, 65 (1955).

² B. W. Batterman, D. R. Chipman, and J. J. DeMarco, *Phys. Rev.* **122**, 68 (1961).

³ J. J. DeMarco, *Phil. Mag.* **15**, 483 (1967).

⁴ M. Järvinen, M. Merisalo, and O. Inkinen, *Phys. Rev.* **178**, 1108 (1968).

⁵ P. A. Doyle and P. S. Turner, *Acta Cryst.* **A24**, 390 (1968).

⁶ R. J. Weiss, *X-Ray Determination of Electron Distributions* (John Wiley & Sons, Inc., New York, 1966).

another and with the RHF values, for the high-order reflections. The BCD results are systematically low, which implies a considerable redistribution of the deep-lying electrons. This has been rejected by Weiss,⁶ who suggested, rather, an experimental error due to the difficulty in resolving high-angle powder peaks. The older BWW results, on the other hand, are considerably closer to the RHF values, although generally higher, while the DM results are lower. The over-all picture is thus one where the measured values disagree with one another and straddle the theoretical predictions. This points more towards experimental inaccuracies than to a true deviation.

The purpose of this work is to clarify the situation for the high-angle peaks and check the magnitude of the deviation for the first two reflections.

EXPERIMENT

We have measured the first nine structure factors of aluminum on an absolute scale by symmetrical reflection from pressed powder samples. The (111), (200), and (220) reflections were measured using monochromatic $\text{Cu } K\alpha$ radiation, and put on an absolute scale by also measuring the incident beam power. Detailed relative intensity measurements were then made on all nine peaks using both monochromatic $\text{Cu } K\alpha$ and nickel-filtered $\text{Cu } K\alpha$ radiation. These measurements were normalized to the absolute measurements of the first three peaks to obtain all nine structure factors absolutely. We shall discuss the absolute and relative measurements separately as well as the methods of preparing the samples.

A. Sample Preparation

The aluminum powder used was J. T. Baker #0446, finer than 325 mesh. Microscopic examination showed a maximum particle size of 8–9 μ , with an average size of about 3 μ . According to mass spectrographic analysis, the only major impurities were 0.1% iron and 0.1% silicon. To ensure that the correct absorption coefficient was used, however, the absorption of a pellet of the sample material was measured. This will be discussed later.

1. Preferred Orientation

Initial investigations were made on samples lightly pressed into recessed holders with a glass plate. The necessity of sliding the glass plate off in order to obtain a smooth surface, however, caused strong preferred orientation. On all samples so made, the (111) reflection was low, while the (200) reflection was somewhat high. This was determined by taking the ratios (111)/(220) and (200)/(220). This is the same preferred orientation seen in all rolled aluminum foils; in ordinary household foil, the (111) peak is almost nonexistent, while the (200) is over twice its normal intensity.

The second method attempted consisted of settling the sample from a slurry of the powder with acetone or xylene. While samples could be made in this way which were free of preferred orientation, the effects of surface roughness could be seen for low-angle reflections. The (111) and (200) form factors were 5–6% below theory, and different samples yielded slightly different intensities for these two peaks. The higher-angle reflections were unaffected.

The samples finally used were formed in a polished 1-in.-diam die under uniaxial pressure varying from 1×10^3 to 5×10^3 psi. Their thickness was from 4 to 6 mm. The intensities of all peaks were independent of forming pressure in this range, and no preferred orientation was observed. Samples formed at more than 5×10^3 psi showed some preferred orientation of the type mentioned above, and thus could not be used. Some samples were measured both before and after light sandblasting and no changes in intensity were observed. If the sample was abraded heavily enough so that the surface became visibly uneven, however, the intensities of the (111) and (200) reflections were found to decrease, as is characteristic of surface roughness.⁷ The samples used in the measurements reported here were not abraded.

2. Extinction, Porosity, and Surface Roughness

Although the 3- μ size of the aluminum powder used should exclude the presence of extinction, an experimental check was performed to eliminate this possibility. Extinction varies strongly with wavelength as well as diffraction angle.⁸ As a result, the ratios of experimental form factors f , such as $f(111)/f(200)$ and $f(200)/f(220)$, which can be obtained directly from relative intensity measurements at different wavelengths using the appropriate multiplicity, polarization, anomalous dispersion, and thermal vibration corrections, are very sensitive to extinction. These ratios were measured using Mo, Cu, and Cr $K\alpha$ radiations and appeared to be wavelength-independent to better than 1% for all of the pellets used. Such a test eliminates the possibility of extinction, and confirms the absence of porosity and surface roughness, since their effects are also wavelength-dependent.⁶

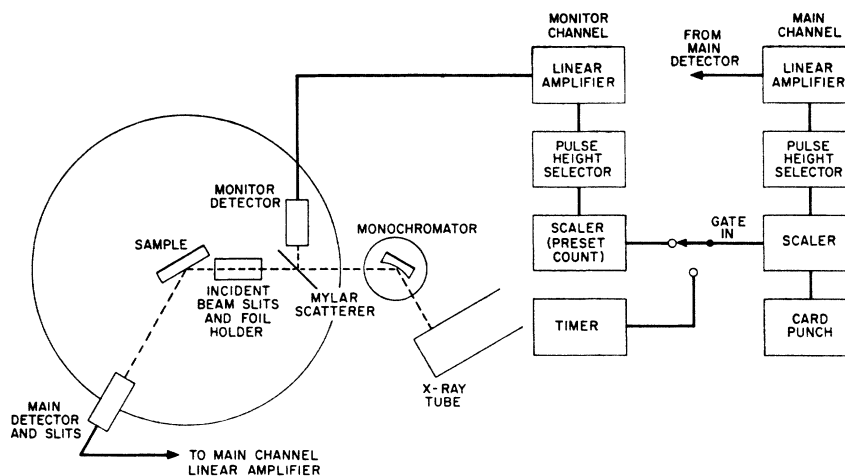
B. Absolute Measurements

The first three Bragg reflections [(111), (200), and (220)] were measured on an absolute scale using monochromatic $\text{Cu } K\alpha$ radiation. These peaks were chosen because they are well separated, have large peak-to-background ratios, and are fairly insensitive to uncertainties in the polarization constant of the monochromator. The method of measurement, as well

⁷ T. Paakkari and P. Suortti, *Acta Cryst.* **A24**, 701 (1968).

⁸ W. H. Zachariasen, *Theory of X-Ray Diffraction in Crystals* (Dover Publications, Inc., New York, 1967).

FIG. 1. Experimental apparatus.



as all of the quantities entering into an absolute scale for the form factor (1), will be discussed in detail.

$$I(s) = \frac{I_0 l N^2 \lambda^3 |F(s)|^2 r_e^2 P(\theta)}{32\pi\mu r}, \quad (1)$$

where $I(s)$ is the diffracted power, s is the diffraction vector [$= |k|/4\pi = (\sin\theta)/\lambda$], θ is the Bragg angle, I_0 is the incident power, l is the detector slit height, N is the number of atoms/volume, λ is the x-ray wavelength, $F(s)$ is the structure factor [$= f^0(s) + \Delta f' + i\Delta f''$], $f^0(s)$ is the atomic form factor, $\Delta f'$ and $\Delta f''$ are the anomalous dispersion corrections, r_e is the classical electron radius ($= e^2/mc^2$), $P(\theta)$ is the Lorentz-polarization factor [$= (1 + K \cos^2 2\theta)/(1 + K) \sin^2 \theta \cos \theta$], K is the monochromator polarization ratio, μ is the linear x-ray absorption coefficient, and r is the radius of the diffractometer.

1. Equipment

The absolute measurements were made on a General Electric XRD-5 diffractometer equipped with a large-focal-spot copper target x-ray tube. The generator was run at 16 kV and 40 mA to eliminate any high-energy harmonics of the characteristic radiation that would be passed by the incident beam monochromator, which was a doubly bent LiF crystal manufactured by Electronics and Alloys, Inc. The crystal was designed to focus 5.73 in. before the sample horizontally and 5.73 in. after the sample vertically. The beam was about 6×3 mm at the sample, and roughly 1 cm square at the detector. Since the curvature of the monochromator crystal limited the vertical spread of the beam at the detector, incident beam measurements were possible without the use of vertical limiting slits. High-resolution Soller slits were used between the monochromator and the sample with the plates normal to the diffraction plane. This was done to eliminate the wings of the radiation coming from the monochromator, since they usually contain small amounts of energy on either side

of the $K\alpha$ lines. The holder for the brass absorbers used to attenuate the beam for incident power measurements was rigidly fastened to the Soller slits. Each foil fit into a slot only a few thousandths of an inch larger than its own thickness to ensure that the absorber would always be in exactly the same position with respect to the incident beam.

An accurately machined brass slit, 1.2° wide in 2θ , was used at the detector for measurements of the Bragg peaks. Its dimensions were measured with an optical comparator, which showed its width to be uniform to 0.1%.

The criteria for proper alignment of the diffractometer were: center of incident beam coincident with diffractometer axis, incident beam centered at 0° in 2θ , and proper location of powder peaks.

In all monochromatic measurements, the incident beam intensity was monitored and used to determine the counting time. A piece of 9-mil Mylar mounted in a rigid brass frame was placed between the monochromator and attenuator holder. The Mylar sheet was oriented roughly 45° to the incident beam (see Fig. 1) and reduced the incident beam intensity by about 27%. A scintillation counter was placed at right angles to the incident beam, and about 4 cm from it, to receive the radiation scattered by the Mylar. Typical counting rates for this monitor were 500 counts/sec. The detector and electronics for the monitor channel were identical to those of the main detector channel.

Both counters were NaI(Tl) scintillation crystals, 1.9 cm in diameter, with Amperex photomultipliers. Hamner NB-18A preamplifiers and General Electric XRD-5 linear amplifiers, pulse-height selectors, and scalars were used. The pulse-height-selector lower limit was set at the minimum between the elastic peak and the low-energy noise, and the upper limit was set on the high-energy side of the peak where the intensity was less than 1% of the center of the peak. With these settings, the dark noise of both channels was about 1 count/sec.

A correction for the nonlinearity of the electronics at high counting rates had to be used. Owing to the "dead time" of the system, the actual counting rate N_T and the observed rate N_0 are related by

$$N_T = N_0 / (1 - N_0 \tau), \quad (2)$$

where τ is the dead time. To determine τ , the absorption ratio of a brass foil was measured at different counting rates, as described by Chipman.⁹ The value of τ determined in this manner was $3.9 \pm 0.4 \mu\text{sec}$. All measured count rates were then corrected by means of Eq. (2). The error in the dead-time correction was included in the error limits of all quantities requiring such a correction.

The output of the monitor scaler was used to directly control the counting time of the main channel scaler. A preset count on the monitor channel triggered the printing of the main scaler. In this manner, any fluctuations in the incident beam intensity were automatically eliminated. Tests of the monitor's effectiveness were made by varying both the x-ray tube current and voltage (between 12 and 16 kV). The main channel output was stable to about 0.2% during these variations (although the counting time per point changed drastically, of course).

2. Measurement of Diffracted Power

The intensities of the first three Bragg peaks were measured using the 1.2° slits previously mentioned. Five points, 1.2° apart in 2θ , were used for each peak, with the middle point centered on the peak. The incident beam intensity was monitored as described above. The central point received about 90% of the peak intensity, with the remaining four points used mainly for background definition. If the five points are labeled $A_1 \cdots A_5$, with the majority of the peak intensity in A_3 , the integrated intensity (including the thermal diffuse scattering contribution) is

$$I = \left(\sum_{i=1}^5 A_i \right) - \frac{5}{2} (A_1 + A_5).$$

The integrated intensities were corrected for thermal diffuse scattering by the method of Chipman and Paskin.¹⁰ The correction was made for the full interval $A_1 \cdots A_5$. Its maximum contribution was 2.4% on the (220) peak.

Correction for the curvature of the Bragg halo ranged from 0.16% on the intensity of the (111) peak to 0.08% for peaks near 90° in 2θ .

3. Attenuation of Incident Beam

In order to keep the incident beam intensity within the counting range where it could be measured ac-

curately, it was necessary to attenuate the beam before making any incident power measurements. This was done using two brass foils, 0.003 and 0.004 in. thick. The absorption of each of these foils was measured separately at counting rates such that the dead-time correction did not exceed 3.5%. The combined foils attenuated the beam by a factor of 2900 ($\pm 0.6\%$).

4. Measurements of Incident Power

A few measurements of incident beam intensity were made by step-counting the beam with the same slits and at the same scan rate used for the diffracted beam. This eliminated the necessity of knowing either the scan rate or slit width, but was more time-consuming and cumbersome than the one-step procedure generally used. The latter consists of removing all detector slits, setting the detector at 0° in 2θ , and measuring the entire beam power at once. (The 1.9-cm scintillation crystal was larger than the 1-cm square beam.) The incident beam was monitored during all measurements. The only disadvantage of this method over using slits is the possibility of different areas of the scintillation crystal having different sensitivity to the x rays. This was unlikely, since the crystals are 98% efficient at this wavelength, but it was checked in two ways. Using a spatially uniform source of x rays, such as the diffuse scattering from a block of commercial boron nitride, a pinhole was moved around the surface of the detector crystal. On some crystals, regions of reduced sensitivity were found. Subsequent visual inspection showed that in all cases the regions corresponded to cloudy areas on the crystal, presumably due to moisture damage. No crystal presenting such irregularities was used. The second method consisted of performing the incident beam and diffracted peak measurements with several different scintillation crystals. The same results were obtained every time.

5. Monochromator Polarization Constant

The (200) reflection of the LiF monochromator was used. This would give a polarization constant of 0.707 if the crystal were perfect, but the possibility of extinction or imperfection made it imperative to measure this constant directly. This was done using a perfect¹¹ germanium crystal and the technique described by Jennings.¹² The value found was 0.753 ± 0.015 . It should be pointed out that the error in $P(\theta)$ is much smaller than the uncertainty in the polarization constant, because of the functional dependence [see Eq. (1)]. The error in $P(\theta)$ ranged from 0.2 to 0.6% for the first three reflections.

⁹ D. R. Chipman, *Acta Cryst.* (to be published).

¹⁰ D. R. Chipman and A. Paskin, *J. Appl. Phys.* **30**, 1998 (1959).

¹¹ By "perfect" we mean having a dislocation density of less than $500/\text{cm}^2$, and showing uniform scattering properties across its surface.

¹² L. D. Jennings, *Acta Cryst.* **A24**, 472 (1968).

6. Wavelength

Using the perfect Ge single crystal, the wavelength distribution of the incident monochromatic beam was obtained and the ratio of the $K\alpha_2$ -to- $K\alpha_1$ contributions determined. It was found to be 49%, very close to the natural ratio of 48%. The average wavelength was evaluated as $1.5411 \pm 0.0002 \text{ \AA}$.

7. Mass Absorption of Aluminum

The spread in published values of the x-ray absorption coefficient of aluminum¹³ at 1.541 \AA is much larger than the level of accuracy needed in this experiment. It was thus necessary to measure the absorption, preferably on the sample material, with an accuracy better than 1%. Measurements were made both on a pressed pellet of the sample material and on very pure aluminum foils.

To get a briquette of the sample powder thin enough to have a measurable transmission and dense enough to be free of holes and thin spots required a pressure of $25 \times 10^3 \text{ psi}$. Several disks, about 0.008 in. thick, were made around this pressure, and were tested for uniform thickness by measuring the absorption at 8 or 10 points across the face. Only one sample was uniform enough for the necessary accuracy. Long counting times (monitored) were used at each of 10 points, and the spread in values was less than 1%. The disk was kept within 2° of normal to the x-ray beam to ensure constant path length through the sample. It was then weighted, and its area was measured with an optical comparator, giving the area mass density ρ_A . The mass absorption coefficient was then evaluated from

$$\mu = -(1/\rho_A) \ln(I/I_0). \quad (3)$$

The value obtained was $50.4 \pm 0.3 \text{ cm}^2/\text{g}$. This is in good agreement with the recent values of 50.4 ± 0.6^{14} and $50.6 \pm 0.5^{15} \text{ cm}^2/\text{g}$.

The correction for the presence of both α_1 and α_2 wavelengths in the x-ray beam⁹ was computed for our foils and found to be less than 0.02%.

8. Miscellaneous Constants

The quantity N^2 in Eq. (1) requires a knowledge of the cell edge in aluminum. The value used was 4.0494 \AA .¹⁵ The slit height l was measured with an optical comparator to 0.01%. The sample-to-slit distance r was measured to 0.1%. The distance was measured to the side of the slits away from the sample as they defined the solid angle seen by the sample.

¹³ G. D. Hughes, J. B. Woodhouse, and I. A. Bucklow, *Brit. J. Appl. Phys.* **2**, 695 (1968).

¹⁴ M. J. Cooper, *Acta Cryst.* **18**, 813 (1965).

¹⁵ H. E. Swanson and E. Tatge, *Natl. Bur. Std. (U.S.) Circ.* **539**, Vol. 1 (1953).

C. Relative Measurements

Relative measurements of the first nine Bragg reflections were made using both nickel-filtered Cu $K\alpha$ radiation and monochromatic Cu $K\alpha$ radiation. The General Electric diffractometer described in Sec. B was used for the monochromatic measurements, the only differences being that detector slits 0.2° wide in 2θ were used, and the same step-counting procedure to be described for the filtered measurements was followed.

1. Equipment for Filtered Measurements

The nickel-filtered measurements were made on a Picker x-ray diffractometer using a Dunlee Microfocus copper target x-ray tube, which was run at 40 kV and 36 mA from a very stable constant potential generator. The rated long-term stability of the system, including x-ray tube, detectors, and all electronics, is 1%, but measurements showed it to be better than 0.5%. 1° divergent slits and 0.5° receiving slits were used, both with accompanying Soller slits. Two 0.7-mil nickel foils were used to filter the Cu $K\beta$ line. The beam size at the sample was 1 cm high and 3 mm wide; the 2.5-cm-diam sample thus intercepted all of the beam even at much lower diffraction angles than were actually used.

The diffractometer was aligned by the method developed for that unit and was then checked for accuracy of location of incident beam and of diffracted powder peaks. The maximum possible misalignment was 0.01° in 2θ .

The detector was a photomultiplier behind a NaI(Tl) scintillation crystal. After linear amplification the pulses were passed through a pulse-height analyzer (PHA). The PHA lower limit was set at the minimum between the dark noise and the $K\alpha$ peak, and the upper limit was set at a point above the peak where the counting rate was less than 5% that of the peak. With these settings, the dark noise was less than 0.5 counts/sec. The dead-time correction was neglected, since it was considerably smaller than the statistical shot noise.

2. Integrated Intensity and Background Determination

The measurements were made by stepping at intervals of 0.02° in 2θ and accumulating counts for a preset time. Each step's total was punched on cards for subsequent computer plotting. Large regions in 2θ were explored on each side of all peaks in order to ensure good background definition. Eventually, graphs having a very large effective time constant were obtained (see Fig. 2) from which appropriate limits of integration were chosen. The background was considered to be linear between these limits, and subtracted from the total intensity, which was obtained by

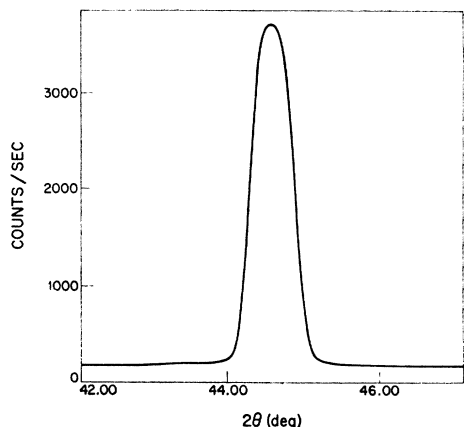


FIG. 2. Computer plot of (200) line shape with data taken at intervals of 0.02° in 2θ . Noise level is smaller than the thickness of the line.

computer integration, and this yielded the peak's intensity.

The procedure is straightforward if the peaks are well separated from one another and from the absorption edges. Two pairs of reflections did not satisfy these conditions: the (311)-(222) and (331)-(420). In both cases the absorption edge of the second line occurred under the first. Correction was made for this by measuring how large a contribution is made to a peak's integrated intensity by inclusion of its absorption edge. The first three peaks were integrated using the background limits which included the absorption edge and those which did not include the absorption edge (Fig. 3). The area included under the absorption edge was found to be $(2.5 \pm 0.1)\%$ of the integrated intensity. This meant that the (222) and the (420) were contributing 2.5% of their intensity to the (311) and (331), respectively. Assuming the basic line shape to be Gaussian, and using the experimental height and half-width, the midpoint between pairs was analytically determined. Each of the four peaks was then integrated separately, and the true intensities obtained by subtracting the (222) and (420) absorption-edge contributions from the (311) and (331), respectively. These final values changed insignificantly when other line shapes such as Lorentzians were assumed. Another

TABLE II. Comparison of our experimental aluminum form factors with theory.

hkl	$ k /4\pi$ (\AA^{-1})	$ F(k) ^2/\mu$		Experi- mental form factor	Theory	
		This work	Jennings		Rela- tivist-ic Hartree- Fock	Rela- tivist-ic Hartree- Fock-Slater
111	0.2138	0.5478	0.548 ± 0.005	8.80 ± 0.06	8.97	9.10
200	0.2470	0.4845	0.485 ± 0.004	8.38 ± 0.06	8.51	8.63
220	0.3493	0.3293	0.334 ± 0.004	7.27 ± 0.06	7.32	7.43
311	0.4094	0.2562		6.66 ± 0.06	6.66	6.78
222	0.4276	0.2365		6.48 ± 0.06	6.47	6.59
400	0.4937	0.1694		5.78 ± 0.06	5.76	5.90
331	0.5381	0.1339		5.33 ± 0.06	5.32	5.46
420	0.5520	0.1239		5.20 ± 0.05	5.18	5.33
422	0.6047	0.0901		4.66 ± 0.05	4.67	4.82

method used was to consider each pair as a single peak and resolve them using the theoretical ratios suitably corrected for the absorption-edge contributions. The results were virtually the same in both cases.

All peaks were counted for times long enough to reduce the statistical uncertainty in the integrated intensity to 0.1%. This includes the uncertainty in the background determination due to counting statistics. The times per peak necessary for this ranged from 2 h for the (111) peak to several days for the very weak ones. Since no incident beam monitor was used for the filtered measurements, however, the true accuracy of the intensities is determined by the stability of the x-ray tube and electronics. As mentioned above, this was found to be about 0.5%. Many of the aluminum peaks were remeasured at different times, bearing out this estimate.

Corrections for thermal diffuse scattering were the same as for the absolute measurements.

D. Data Analysis

This series of experiments yielded two sets of integrated intensities. The relative intensities of all nine peaks, which are an average of both monochromatic and filtered measurements on several samples, were put on an absolute scale by normalizing $|F(hkl)|^2/\mu$ for the first three peaks to their absolute values. These absolute values are also the average of measurements on several samples. Knowing μ , the nine absolute structure factors were obtained. These were then corrected for thermal vibration using a Debye-Waller parameter of $0.894 \pm 0.009 \text{ \AA}^2$ based on a Debye temperature of $387 \pm 2^\circ\text{K}$ determined by recent x-ray³ and neutron¹⁶ measurements. This yielded the quantity

$$|F(s)|^2 = [f^0(s) + \Delta f']^2 + (\Delta f'')^2,$$

which was corrected for anomalous dispersion using

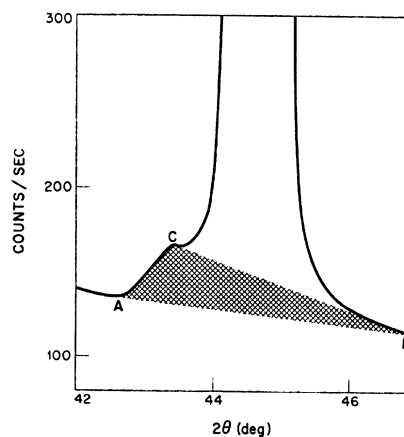


FIG. 3. Background integration limits which include (A-B) and exclude (C-B) the absorption-edge contribution. (Expanded scale of Fig. 2).

¹⁶ D. L. McDonald, *Acta Cryst.* **23**, 185 (1967).

Cromer's¹⁷ values $\Delta f' = 0.19$ and $\Delta f'' = 0.27$ to give the solid-state form factors $f^0(s)$.

RESULTS AND DISCUSSION

Our results are compared with theoretical calculations in Table II and Fig. 4. The uncertainty intervals given correspond to the combination of all errors in both the absolute and relative measurements. The results are lower than the RHF values for the first two structure factors [(111) and (200)], as are those of all previous observations. The other Fourier components, however, agree very closely with the free-atom RHF calculation and depart in various ways from the earlier experiments. Our measurements present, in general, a smaller uncertainty than the previous ones, and from the over-all experimental picture, one must conclude that the probable values are very close to the RHF theory. In other words, the electrons close to the nucleus are free-atom-like.

We have also compared our results to a calculation in which Slater's¹⁸ approximation to the exchange potential is used. Cromer and Waber¹⁹ obtained atomic form factors (column 7) from relativistic wave functions based on this approximation. These values disagree with our results for all reflections. This discrepancy has been discussed elsewhere²⁰ and is due partly to the fact that the $\rho^{1/3}$ approximation seems to depend on having the charge density varying slowly in space.^{18,21,22} Slater pointed out to us, however, that the use of an adjustable parameter multiplying the exchange potential yields solutions very close to the true Hartree-Fock.

For the first two reflections, the departure of our results from the RHF values is smaller than that reported by any of the previous workers. (It should be pointed out that all of the usual sources of error such as extinction, porosity, or surface roughness would decrease rather than increase the intensities of these peaks.) Furthermore, a recent measurement of the (111) form factor by means of high-energy electron diffraction²³ gave 8.87 ± 0.08 , in agreement with our value. The departure from theory is still large enough,

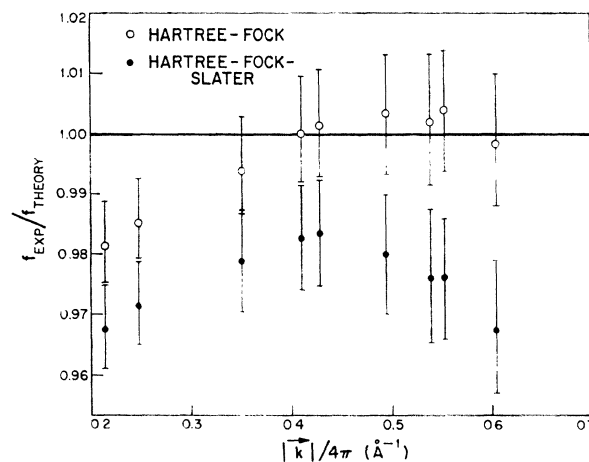


FIG. 4. Ratio of experimental to theoretical form factors for RHF and RHFS theories.

however, to ask if a simple redistribution of the valence electrons can explain it or whether core expansion is necessary. It turns out that any of a number of plausible valence-electron redistributions can represent our results. A screening model, for instance, turned out to be very successful and is discussed at length elsewhere.²⁴ This does not prove that the core electrons are unaffected by the crystalline field, but it shows that these data do not require such an effect.

In conclusion, our measurements have confirmed the existence of a solid-state effect in the scattering of Al, most likely due to a redistribution of the outer (valence) electrons alone. They have also shown that the free-atom RHF calculation describes closely the solid-state form factor of Al at high values of the scattering vector

ACKNOWLEDGMENTS

The authors would like to thank L. D. Jennings for many fruitful discussions on all phases of the work, as well as for performing independent measurements on one of our samples. We would also like to thank T. A. Kaplan, M. M. Litvak, and H. J. Zeiger for many valuable suggestions, and C. H. Anderson for preparing the samples and helping with most of the measurements.

¹⁷ D. T. Cromer, *Acta Cryst.* **18**, 17 (1965).

¹⁸ J. C. Slater, *Phys. Rev.* **81**, 385 (1951).

¹⁹ D. T. Cromer and J. T. Waber, *Acta Cryst.* **18**, 104 (1965).

²⁰ P. M. Raccach and V. E. Henrich, *J. Quantum Chem.* (to be published).

²¹ R. Gaspar, *Acta Phys. Acad. Sci. Hung.* **3**, 263 (1954).

²² W. Kohn and L. J. Sham, *Phys. Rev.* **140**, A1133 (1965).

²³ D. Watanabe, R. Uyeda, and A. Fukuhara, *Acta Cryst.* **A25** 138 (1969).

²⁴ P. Ascarelli and P. M. Raccach (to be published).